$$k = (2\pi/\hbar)|V^2|(\mathrm{FCWD}) \quad (1a)$$

$$\mathrm{FCWD} = (4\pi\lambda_s k_B T)^{-1/2} \sum_{w=0}^{\infty} (e^{-S} S^w / w!) \exp\{-[(\lambda_s + \Delta G^\circ + wh\nu)^2 / 4\lambda_s k_B T]\} \quad (1b)$$

$$S = \lambda_v / h\nu \quad (1c)$$

Equation 1 is based on the golden rule (eq 1a) and incorporates the quantum-mechanical treatment of high-frequency modes of the donor and acceptor groups, together with the classical treatment of the solvent modes.[4,3c] The parameters were derived from room-temperature measurements on QSB, ClQSB, and six others with different acceptor groups providing a range from −0.06 to −2.5 eV. Fitting these data to eq 1 provided the solvent reorganization energy (λ_s = 0.75 eV for MTHF), the reorganization energy (λ_v = 0.45 eV) of the high-frequency vibrational modes, here represented by a single average skeletal vibration of 1500 cm^{-1}, and the coupling matrix element V (6.2 cm^{-1}).[3d] The parameters were further confirmed by measuring the temperature dependence of k_{intra} of NSB (N = 2-naphthyl) and λ_s of MTHF.[6] However, because of the weak exoergicity (ΔG° = −0.06 eV), the high-frequency mode is restricted to w = 0, making the part of eq 1 that depends on temperature equal to the classical Marcus expression.

According to eq 1, the rates are very weakly dependent on temperature because of the quantum-mechanical nature of the high-frequency modes. These modes are "frozen" in our temperature range. Their Franck–Condon factors are not improved by increasing temperature in our range because of nuclear tunneling in these modes. The nuclear tunneling makes the high-frequency modes efficient at disposing the excess energy in these highly exoergic reactions. In addition, λ_s of MTHF increases by 20% from 100 to −94 °C,[6] which is responsible for the slightly negative activation energies (≈−0.18 kcal/mol for ClQSB). If λ_s were independent of temperature, the rates would still have been predicted to be almost independent of temperature, but with a very weakly positive activation energy (0.5 kcal/mol).

For the same donor–acceptor pairs, the intermolecular rate constants (lower Figure 1) are quite sensitive to temperature but insensitive to ΔG°. This is because k_{inter} is primarily determined by diffusion as demonstrated by the excellent fit of the data to the phenomenological VTF equation:[7] $k = k_0 \exp[-E_0/(T - T_0)]$ with E_0 = 0.40 K^{-1} and T_0 = 100 ± 20 K. This is another demonstration of how the unique features of the inverted region are buried in rate-limiting transport processes in bimolecular reactions.

In conclusion, while the Marcus theory in its classical form describes the temperature dependence of ET at least qualitatively in the normal region, the present study finds it to be inadequate in the inverted region. Here, it is essential to include a quantum-mechanical treatment of high-frequency modes. In kinetic terms, the classical theory attributes the inverted region to an increasing activation energy in the exponential term of the rate equation, while because of nuclear tunneling it is the decreasing preexponential factor that is primarily responsible for the diminishing rate. Other evidence for the necessity of quantum modes in ET processes is abundant.[8a,9,10] The observations reported here resemble the temperature-independent ET processes in photosynthetic reaction centers[8] and may shed some light on the understanding of this important problem.

Acknowledgment. We are indebted to Radhika Bal for resynthesizing some of the compounds and to Professor R. A. Marcus for helpful comments on the role of tunneling in the inverted region. Work at Argonne was supported by the Office of Basic Energy Sciences, Division of Chemical Science, U.S. Department of Energy, under Contract No. W-31-109-ENG-38. Work at the University of Chicago was supported by NSF Grant CHE-8520326.

(6) Liang, N.; Miller, J. R.; Closs, G. L. *J. Am. Chem. Soc.* **1989**, *111*, 8740.
(7) (a) Vogel, H. *Phys. Z.* **1921**, *22*, 645. (b) Fulcher, G. S. *J. Am. Chem. Soc.* **1925**, *8*, 339. (c) Tammann, G.; Hesse, G. *Z. Anorg. Allg. Chem.* **1926**, *156*, 245. (d) Recent review: Fredrickson, G. H. *Annu. Rev. Phys. Chem.* **1988**, *39*, 149.
(8) (a) Gunner, M. R.; Dutton, P. L. *J. Am. Chem. Soc.* **1989**, *111*, 3400. (b) Kirmaier, C.; Holten, D.; Parson, W. W. *Biochim. Biophys. Acta* **1985**, *810*, 33. (c) Schenck, C. C.; Parson, W. W.; Holten, D.; Windsor, W. W.; Sarai, A. *Biophys. J.* **1981**, *36*, 479.
(9) Marcus, R. A. *J. Phys. Chem.* **1989**, *93*, 3078.
(10) Penfield, K. W.; Miller, J. R.; Paddon-Row, M. N.; Cotsaris, E.; Oliver, A. M.; Hush, N. S. *J. Am. Chem. Soc.* **1987**, *109*, 5061.

Feasibility of a "Building-Block" Approach to Higher Nuclearity Mn/O/RCO_2^- Aggregates: Directed Conversion of an $[Mn_4O_2]$ to an $[Mn_8O_4]$ Complex

Eduardo Libby, Kirsten Folting, John C. Huffman, and George Christou*[,1]

Department of Chemistry and the Molecular Structure Center Indiana University, Bloomington, Indiana 47405
Received January 19, 1990

In recent years we have been reporting our progress toward developing oxide-bridged Mn carboxylate chemistry.[2] Efforts have been directed primarily toward di- and tetranuclear species to obtain potential models of the Mn units within certain Mn biomolecules.[2] We, and others, have occassionally encountered higher nuclearity products, and structurally characterized species include Mn_6,[3] Mn_9,[4] Mn_{10},[5] and Mn_{12}.[6] In parallel, other groups have reported high nuclearity Fe carboxylates, Fe_6,[7] Fe_8,[8] Fe_{11},[9] and $Fe_{16}M$ (M = Co, Mn).[10] In all cases, it is probably fair to say that serendipity has provided a helping hand, in that reactions were under thermodynamic control and the precise nuclearity could not have been predicted from the reagents employed. Higher nuclearity species are important for a variety of reasons, including providing insights into the assembly of the polynuclear core of the ferritin protein[11] and understanding the variation of magnetic exchange interactions as a function of nuclearity and metal oxidation state.[2] The latter has been particularly interesting for Mn where ferromagnetic interactions have occasionally led to high spin ground states. For example, $Mn_{12}O_{12}(O_2CPh)_{16}(H_2O)_4$ has an S = 14 ground state, and we have commented on the potential of such species as precursors to molecular ferromagnets.[6a] Given this importance of high-nuclearity species and the serendipitous nature of their discovery to date, we felt it important to overcome this lack of control and develop methodology for their rational synthesis. One attractive approach is to link together, in a controlled manner, smaller nuclearity "building blocks" derived from available smaller nuclearity species. Preliminary efforts have

(1) Alfred P. Sloan Research Fellow, 1987–1991. Camille and Henry Dreyfus Teacher-Scholar, 1987–1992.
(2) Christou, G. *Acc. Chem. Res.* **1989**, *22*, 328 and references therein.
(3) (a) Schake, A. R.; Vincent, J. B.; Li, Q.; Boyd, P. D. W.; Folting, K.; Huffman, J. C.; Hendrickson, D. N.; Christou, G. *Inorg. Chem.* **1989**, *28*, 1915. (b) Baikie, A. R. E.; Howes, A. J.; Hursthouse, M. B.; Quick, A. B.; Thornton, P. J. *J. Chem. Soc., Chem. Commun.* **1986**, 1587. (c) Gerbeleu, N. V.; Batsanov, A. S.; Timko, G. A.; Struchkov, Y. T.; Inrichan, K. M.; Popovich, G. A. *Dokl. Akad. Nauk SSSR* **1987**, *294*, 256.
(4) Christmas, C.; Vincent, J. B.; Chang, H.-R.; Huffman, J. C.; Christou, G.; Hendrickson, D. N. *J. Am. Chem. Soc.* **1988**, *110*, 823.
(5) Hagen, K. S.; Armstrong, W. H.; Olmstead, M. M. *J. Am. Chem. Soc.* **1989**, *111*, 774.
(6) (a) Boyd, P. D. W.; Li, Q.; Vincent, J. B.; Folting, K.; Chang, H.-R.; Streib, W. E.; Huffman, J. C.; Christou, G.; Hendrickson, D. N. *J. Am. Chem. Soc.* **1988**, *110*, 8537. (b) Lis, T. *Acta Crystallogr., Sect. B* **1980**, *B36*, 2042. (c) Luneau, D.; Savariault, J.-M.; Tuchagues, J.-P. *Inorg. Chem.* **1988**, *27*, 3912.
(7) (a) Micklitz, W.; Bott, S. G.; Bentsen, J. G.; Lippard, S. J. *J. Am. Chem. Soc.* **1989**, *111*, 372. (b) Micklitz, W.; Lippard, S. J. *Inorg. Chem.* **1988**, *27*, 3067. (c) Batsanov, A. S.; Struchkov, Y. T.; Timko, G. A. *Koord. Khim.* **1988**, *14*, 266.
(8) Wieghardt, K.; Pohl, K.; Jibril, I.; Huttner, G. *Angew. Chem., Int. Ed. Engl.* **1984**, *23*, 77.
(9) Gorun, S. M.; Papaefthymiou, G. C.; Frankel, R. B.; Lippard, S. J. *J. Am. Chem. Soc.* **1987**, *109*, 3337.
(10) Micklitz, W.; Lippard, S. J. *J. Am. Chem. Soc.* **1989**, *111*, 6856.
(11) (a) Theil, E. C. *Annu. Rev. Biochem.* **1987**, *56*, 289. (b) Crichton, R. R. *Angew. Chem., Int. Ed. Engl.* **1973**, *12*, 57.

0002-7863/90/1512-5354$02.50/0

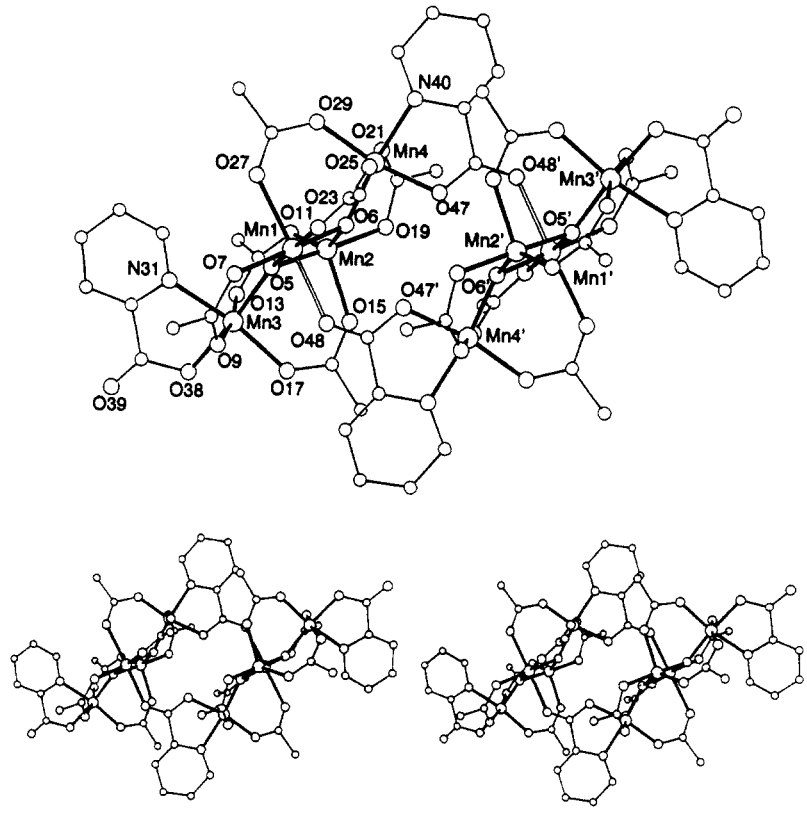

Figure 1. Labeled structure and stereoview of complex **2**. To avoid congestion, not all symmetry-equivalent atoms have been labeled. The μ_3-O atoms are O5, O5′, O6, and O6′. Selected distances (Å): Mn1···Mn2, 2.876 (7); Mn1···Mn3, 3.450 (7); Mn1···Mn4, 3.309; Mn2···Mn3, 3.248 (7); Mn2···Mn4, 3.300 (7); Mn1–O5, 1.932 (19); Mn2–O5, 1.863 (20); Mn3–O5, 1.872 (19); Mn1–O6, 1.904 (20); Mn2–O6, 1.882 (20); Mn4–O6, 1.859 (19); Mn1–O48, 2.236 (19); Mn4–O47, 1.946 (20); Mn3–N31, 2.060 (25); Mn4–N40, 2.038 (23); Mn3–O38, 1.905 (20); Mn1–O7, 1.956 (23); Mn1–O23, 1.939 (23); Mn1–O27, 2.222 (21); Mn2–O11, 1.997 (21); Mn2–O15, 2.061 (20); Mn2–O19, 1.947 (21); Mn3–O9, 2.134 (20); Mn3–O13, 2.213 (23); Mn3–O17, 1.970 (20); Mn4–O21, 2.237 (23); Mn4–O25, 2.126 (20); Mn4–O29, 1.927 (20).

employed $(NBu^n_4)[Mn_4O_2(OAc)_7(pic)_2]$ (**1**; picH = picolinic acid), which is available in large amounts.[12] We reasoned that removal of one AcO^- with Me_3SiCl[13] could yield the coordinatively unsaturated "fragment" $[Mn_4O_2(OAc)_6(pic)_2]$ which *might* dimerize to a nuclearity of eight. We report that this approach does indeed yield such an octanuclear product $Mn_8O_4(OAc)_{12}(pic)_4$ (**2**).

Treatment of complex **1** with 1 equiv of Me_3SiCl in distilled MeCN under N_2 causes a color change from dark red to purple-brown. Layering the filtered solution with Et_2O gave well-formed black crystals of **2** in 24% yield. The structure[14] is shown in Figure 1. The discrete molecule lies on an inversion center. Two $Mn_4O_2(OAc)_6(pic)_2$ fragments have dimerized via the formation of two interfragment linkages employing the picolinate oxygens O48 and O48′ which were not bound to Mn in complex **1**. Only these two bonds hold the fragments together (unshaded in Figure 1 for emphasis). Atoms Mn1, Mn3, and Mn4 are six-coordinate and essentially octahedral, whereas Mn2 is five-coordinate and essentially trigonal bipyramidal (O5–Mn2–O19, 175.2°). The six-coordinate high-spin (d^4) Mn^{III} centers are Jahn–Teller (JT) distorted, and for Mn1, the interfragment linkage

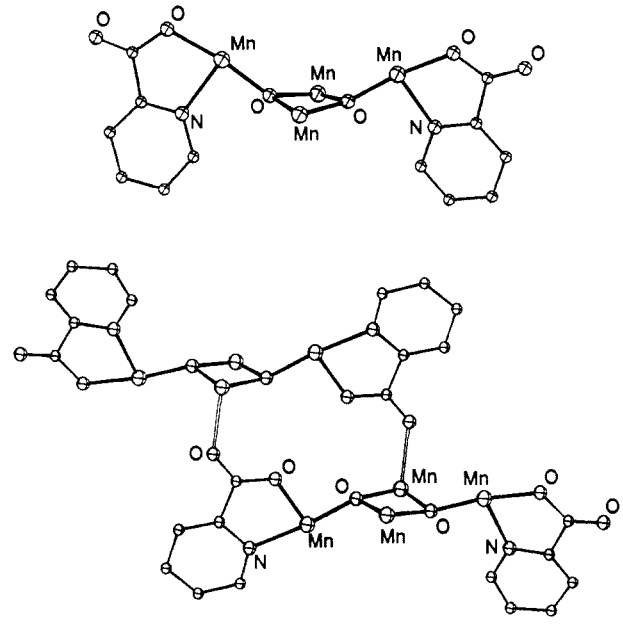

Figure 2. The Mn/O/pic cores of complexes **1** and **2** emphasizing structural changes on dimerization of the $[Mn_4O_2(pic)_2]$ core and the interfragment connections.

(12) Libby, E.; Huffman, J. C.; Christou, G., unpublished results. This antiferromagnetically coupled complex has the same structure as $[Mn_4O_2(OAc)_7(bpy)_2](ClO_4)$ except that chelating picolinate groups replace the chelating bipyridine groups; see: Vincent, J. B.; Christmas, C.; Chang, H.-R.; Huffman, J. C.; Hendrickson, D. N.; Christou, G. *J. Am. Chem. Soc.* **1989**, *111*, 2086.

(13) (a) Green, M. L. H.; Parkin, G.; Bashkin, J.; Fail, J.; Prout, K. *J. Chem. Soc., Dalton Trans.* **1982**, 2519. (b) McCarley, R. E.; Ryan, T. R.; Torardi, C. C. *ACS Symp. Ser.* **1981**, *155*, 41.

(14) Crystallographic data at −157 °C: monoclinic, space group $P2_1/n$; a = 11.276 (5) Å, b = 26.159 (11) Å, c = 11.671 (5) Å, β = 93.11 (2)°, Z = 2; $R(R_w)$ = 8.71(8.28%) with 1364 unique reflections with $F > 3.00\sigma(F)$. All non-hydrogen atoms were readily located. Due to poor diffraction and the small number of data (48 independent atoms), only the Mn atoms were refined anisotropically (212 refined parameters). Hydrogen atoms in fixed, idealized positions were included in the final refinement cycles. Difference maps showed at least five atoms assigned to lattice solvent molecules that were badly disordered; five atoms were included in the final cycles. Analytical data support the presence of lattice MeCN and H_2O molecules from the hygroscopic nature of dried solid. Calculated for $1 \cdot {}^3/_2MeCN \cdot 5H_2O$: C, 33.1; H, 3.6; N, 4.2; Mn, 23.7. Found: C, 33.2; H, 3.4; N, 4.0; Mn, 23.2. IR data (Nujol mull): 3430 (w, br), 3077 (w), 2255 (w), 1682 (m), 1644 (s), 1595 (s), 1568 (s), 1343 (s), 1331 (s), 1294 (s), 1261 (w), 1161 (m), 1097 (w), 1051 (m), 1028 (m), 938 (w), 858 (w), 768 (w), 718 (m), 693 (m), 677 (m), 662 (s), 646 (s), 615 (s), 465 (m).

(Mn1-O48) and Mn1-O27 are the two axially elongated bonds (2.236 (19) and 2.222 (21) Å, respectively). The Mn1-O48 distance (2.236 (19) Å) is similar to the lengths of other JT-elongated Mn-O bonds in **2** (2.126 (20)-2.237 (23) Å). A comparison of the core structures of **1** and **2** is provided in Figure 2. The top half shows the Mn_4O_2 "butterfly" structure in **1** and the disposition of its pic^- ligands. The bottom half shows the $Mn_8O_4(pic)_4$ portion of **2**. Note that, in **1**, both of the μ_3-O atoms are trans to picolinate oxygens while, in **2**, some μ_3-O atoms are also trans to picolinate nitrogen atoms. This can be rationalized as a consequence of the need to accommodate the new interfragment Mn-O bonds. Also, the Mn_4 units in **2** are no longer in a "butterfly" arrangement. Apart from these small structural changes, we emphasize that the $[Mn_4O_2(OAc)_6(pic)_2]$ fragments of **2** are essentially identical with that in **1** vis-à-vis their formulation, gross structural arrangement, and metal oxidation level (all Mn^{III}). This is to be contrasted with the reductive dimerization of $Mn_3O(O_2CPh)_6(py)_2(H_2O)$ (Mn^{II}, $2Mn^{III}$) to $Mn_6O_2(O_2CPh)_{10}(py)_2(MeCN)_2$ ($4Mn^{II}$, $2Mn^{III}$) where the average Mn oxidation level decreases and the two $[Mn_3(\mu_3\text{-}O)]$ cores fuse to a $[Mn_6(\mu_4\text{-}O)_2]$ core.[3a] This is better described as a "cluster condensation" reaction[15] with the $[Mn_3O]$ cores no longer retaining their original identity. This is distinctly different from the conversion of **1** to **2** where no fusion of the two $[Mn_4O_2]$ cores has occurred and which we prefer to call a "building-block" aggregation.

The conversion of **1** to **2** (eq 1) can be rationalized as follows: removal of the carboxylate group bridging central Mn atoms Mn1 and Mn2 yields two five-coordinate centers, one of which is converted back to six-coordination via the new interfragment linkages (Mn1-O48 and its symmetry-related partner) (Figure 2) whereas Mn2 and Mn2′ remain five-coordinate. Note that

$$2Mn_4O_2(OAc)_7(pic)_2^- + 2Me_3SiCl \rightarrow [Mn_4O_2(OAc)_6(pic)_2]_2 + 2Me_3SiOAc + 2Cl^- \quad (1)$$

complex **2** still possesses two pic O atoms not bound to Mn (O39). In principle, carboxylate removal from **2** might yield further aggregation via conversion of O39 to a bridging mode (currently under investigation).

We recognize that formation of **2** from **1** relies on the picolinate and its flexibility in converting from η^2 to $\eta^2{:}\eta^1{:}\mu_2$. Since other $Mn/O/RCO_2^-$ complexes do not possess pic^- ligands, similar transformations are ruled out. Nevertheless, the aggregation of fragments generated from carboxylate abstraction has the potential for general application either with deliberately added bridging ligands or with bound RCO_2^- groups themselves converting from μ_2 to μ_3 or μ_4 modes for interfragment linking.[16] With the feasibility of linking Mn_4O_2 units established, we are investigating application of this approach to the linking of ferromagnetically coupled species such as $Mn_4O_3Cl_4(OAc)_3(py)_3$[17] ($S = {}^9/_2$) and $Mn_{12}O_{12}(O_2CPh)_{16}(H_2O)_4$ ($S = 14$) and determining the magnetic properties of higher nuclearity products.

Acknowledgment. This work was supported by the National Science Foundation (CHE-8808019).

Supplementary Material Available: Tables of fractional coordinates, thermal parameters, and bond distances and angles of **2** (8 pages). Ordering information is given on any current masthead page. A complete MSC structure report is available on request from the Indiana University Chemistry Library.

(15) (a) Fenske, D.; Ohmer, J.; Hachgenei, J.; Merzweiler, K. *Angew. Chem., Int. Ed. Engl.* **1988**, *27*, 1277. (b) Shibahara, T.; Akashi, H.; Kuroya, H. *J. Am. Chem. Soc.* **1988**, *110*, 3313. (c) Shibahara, T.; Yamamoto, T.; Kanadani, H.; Kuroya, H. *J. Am. Chem. Soc.* **1987**, *109*, 3495. (d) Saito, T.; Yamamoto, N.; Yamagata, T.; Imoto, H. *J. Am. Chem. Soc.* **1988**, *110*, 1646. (e) Saito, T.; Yoshikawa, A.; Yamagata, T.; Imoto, H.; Unoura, K. *Inorg. Chem.* **1989**, *28*, 3588.

(16) Carboxylates in μ_3 and μ_4 modes are known; see refs 3 and 6c.

(17) Li, Q.; Vincent, J. B.; Libby, E.; Chang, H.-R.; Huffman, J. C.; Boyd, P. D. W.; Christou, G.; Hendrickson, D. N. *Angew. Chem., Int. Ed. Engl.* **1988**, *27*, 1731.

Shape-Selective Olefin Epoxidation Catalyzed by Manganese Picnic Basket Porphyrins

James P. Collman,* Xumu Zhang, Robert T. Hembre, and John I. Brauman

Department of Chemistry, Stanford University
Stanford, California 94305-5080

Received January 2, 1990

We have previously described the synthesis and characterization of the "picnic basket" porphyrins, which have a rigid cavity of variable dimensions on one face of the porphyrin ring.[1] Using ruthenium derivatives, we were able to control the regiochemistry of axial ligand coordination and to prepare stable dioxygen and dinitrogen complexes.[2] However, the picnic basket system was designed to effect catalytic, shape-selective oxygenations[3] and thus to mimic the enzyme family cytochrome P-450. Our early attempts to epoxidize olefins using manganese derivatives and iodosylbenzene failed to achieve shape selectivity. We were unable to seal the outside of the cavity by blocking the open face of the porphyrin with bulky *neutral* axial ligands such as 3,5-disubstituted imidazoles. Olefins were epoxidized on the open face of the porphyrin. Thus, these catalysts failed to show shape selectivity in the competitive epoxidation of olefin pairs.

We now describe conditions that result in catalytic olefin epoxidation within the cavities of a series of manganese picnic basket porphyrins. We have achieved substrate selectivities that reflect an interplay between the dimensions of the cavity vis-à-vis the shape of the olefin substrate. The solution to this problem involves the use of a bulky, *anionic* axial ligand and acetonitrile as a solvent with iodosylbenzene as the oxidant[4] (eq 1).

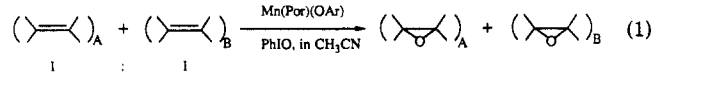

(1)

Our results are summarized in Table I. Very slow epoxidation is observed when the C_2 and C_4 baskets **1** and **2** are used (Figure 1). Apparently, a small amount of reaction occurs at the open face. In these cases the cavities are too restricted for reaction to occur inside. The C_6 basket, **3**, shows a dramatic selectivity as illustrated for *cis*-2-octene competing with *trans*-β-methylstyrene (70:1) and *cis*-2-octene with *cis*-cyclooctene (67:1). The flat, rigid xylyl basket, **6**, shows a slightly lower selectivity with *cis*-2-octene versus *trans*-β-methylstyrene (29:1) but dramatic shape selectivity for *cis*-2-octene versus tub-shaped *cis*-cyclooctene (>1000:1). The modest, inverted selectivities of the hindered open face tetramesitylporphyrin are provided for contrast. The selectivity within the C_8 basket, **4** falls sharply, giving ratios of 12.7:1

(1) Collman, J. P.; Brauman, J. I.; Fitzgerald, J. P.; Hampton, P. D.; Naruta, Y.; Michida, T. *Bull. Chem. Soc. Jpn.* **1988**, *61*, 47.

(2) (a) Collman, J. P.; Brauman, J. I.; Fitzgerald, J. P.; Hampton, P. D.; Naruta, Y.; Sparapany, J. W.; Ibers, J. A. *J. Am. Chem. Soc.* **1988**, *110*, 3477. (b) Collman, J. P.; Brauman, J. I.; Fitzgerald, J. P.; Sparapany, J. W.; Ibers, J. A. *J. Am. Chem. Soc.* **1988**, *110*, 3486.

(3) For earlier examples of shape-selective oxygenations, see: (a) Groves, J. T.; Nemo, T. E. *J. Am. Chem. Soc.* **1983**, *105*, 5786. (b) Suslick, K. S.; Cook, B. R.; Fox, M. M. *J. Chem. Soc., Chem. Commun.* **1985**, 580. (c) Suslick, K. S.; Cook, B. R. *J. Chem. Soc., Chem. Commun.* **1987**, 200. (d) Cook, B. R.; Reinert, T. J.; Suslick, K. S. *J. Am. Chem. Soc.* **1986**, *108*, 7281. (e) Collman, J. P.; Brauman, J. I.; Meunier, B.; Hayashi, T.; Kodadek, T.; Raybuck, S. A. *J. Am. Chem. Soc.* **1985**, *107*, 2000. (f) De Carvalho, M.-E.; Meunier, B. *Nouv. J. Chim.* **1986**, *10*, 223. (g) Mahy, J.-P.; Bedi, G.; Battioni, P.; Mansuy, D. *Nouv. J. Chim.* **1989**, *13*, 651. (h) Groves, J. T.; Newmann, R. *J. Am. Chem. Soc.* **1987**, *109*, 5045. (i) Nappa, M. J.; Tolman, C. A. *Inorg. Chem.* **1985**, *24*, 4711. (j) Herron, N.; Stucky, G. D.; Tolman, C. A. *J. Chem. Soc., Chem. Commun.* **1986**, 1521. (k) Herron, N.; Tolman, C. A. *J. Am. Chem. Soc.* **1987**, *109*, 2837.

(4) (a) To 4 μmol of Mn(Por)X (X = Br, Cl) in 2.5 mL of CH_3CN was added 20 equiv of $Et_2OLi(OAr)$. The solution was stirred at room temperature until the porphyrin Soret at 454 nm completely developed. $Olefin_A$ (125 equiv), $olefin_B$ (125 equiv), and PhIO (55 equiv) with a GC standard (nonane or dodecane) were then added. The epoxidation products were measured by GC as a function of time. With the catalysts Mn(C_6PBP)(OAr) and Mn(PXYLPBP)(OAr), the epoxidation yield of *cis*-2-octene based on PhIO is about 50–75% in 1 h. (b) The epoxidation rate with the catalysts Mn(C_2PBP)(OAr) and Mn(C_4PBP)(OAr) is at least 15 times slower than with Mn(C_6PBP)(OAr).

0002-7863/90/1512-5356$02.50/0